

## Measuring the mass, density, and size of particles and cells using a suspended microchannel resonator

Michel Godin, Andrea K. Bryan, and Thomas P. Burg

Biological Engineering Department, Massachusetts Institute of Technology, Cambridge, Massachusetts 02139-4307, USA

Ken Babcock

Affinity Biosensors, Santa Barbara, California 93117, USA

Scott R. Manalis<sup>a)</sup>

Biological Engineering and Mechanical Engineering Departments, Massachusetts Institute of Technology, Cambridge, Massachusetts 02139-4307, USA

(Received 25 July 2007; accepted 4 September 2007; published online 21 September 2007)

We demonstrate the measurement of mass, density, and size of cells and nanoparticles using suspended microchannel resonators. The masses of individual particles are quantified as transient frequency shifts, while the particles transit a microfluidic channel embedded in the resonating cantilever. Mass histograms resulting from these data reveal the distribution of a population of heterogeneously sized particles. Particle density is inferred from measurements made in different carrier fluids since the frequency shift for a particle is proportional to the mass difference relative to the displaced solution. We have characterized the density of polystyrene particles, *Escherichia coli*, and human red blood cells with a resolution down to  $10^{-4}$  g/cm<sup>3</sup>. © 2007 American Institute of Physics. [DOI: 10.1063/1.2789694]

Nano- and microscale particles and colloidal solutions are central to numerous applications in industrial manufacturing, nanotechnology, and the life sciences. The suspended microchannel resonator (SMR) allows the direct measurement of the absolute mass of individual particles,<sup>1</sup> complementing other techniques currently used for particle size analysis such as light scattering and disk centrifuge sedimentation.<sup>2</sup> We show here that in addition to mass, the SMR measures particle density, which makes it a unique instrument in particle metrology that may provide fundamental information to particulate engineering, as well as to the analysis and diagnostics of cells and organelles.

An SMR sensor comprises a silicon microfluidic channel enclosed in a cantilever geometry that is driven into mechanical resonance [Fig. 1(a)]. The sensor is encapsulated in a vacuum environment and has a quality factor between 8000 and 15 000. The resonant frequency of the sensor can be measured to a few parts per 10<sup>9</sup>, yielding a mass resolution of  $\sim 1$  fg ( $10^{-15}$  g). The experimental setup has been described in detail elsewhere.<sup>1</sup>

The mass of a particle in transit through the SMR channel [Fig. 1(a)] is measured as a transitory resonant frequency shift.<sup>1</sup> The mass distribution of particles in solution is determined by accruing multiple sequential measurements of individual particles. Because the resonant frequency of the cantilever is determined by the total mass, including that of the fluid and of a suspended particle, the SMR measures the difference in mass of a particle with respect to that of the displaced fluid,  $M_d = V(\rho_p - \rho_f)$ , where  $V$  is the particle's volume, and  $\rho_p$  and  $\rho_f$  are the densities of the particle and of the carrier fluid, respectively. The radius of a particle  $R$  assumed to be spherical is determined from  $V = (4/3)\pi R^3$ .

The differential mass  $M_d$  is positive when the particle density is larger than that of the surrounding solution, and it is negative when the particle is buoyant in the solution. To illustrate the effect of solution density on the measured differential mass, a mixture of 99.5 nm gold ( $\rho_p \approx 19.3$  g/cm<sup>3</sup>) and 708.6 nm polystyrene ( $\rho_p \approx 1.05$  g/cm<sup>3</sup>) nanoparticles at a concentration of 10<sup>8</sup> particles/ml was flowed through the resonator. Figure 1(b) reveals that both the gold and the polystyrene nanoparticles have positive differential masses in phosphate buffered saline (PBS) ( $\rho_f \approx 1.0$  g/cm<sup>3</sup>), and the average frequency shift for the mixture is  $-25 \pm 3$  mHz. While the masses of the gold (9.8 fg) and of the polystyrene (195.6 fg) particles differ significantly, their differential masses with respect to the carrier fluid (PBS) are both approximately 9 fg. The resulting mass histograms overlap, and the transitory frequency shifts are indistinguishable. However, when the same mixture was measured in a 44% glycerol solution ( $\rho_f \approx 1.1$  g/cm<sup>3</sup>), the differential mass of each particle ( $-9$  fg for polystyrene and  $+9$  fg for gold) is now clearly distinguishable [Fig. 1(c)], and the resulting histograms are clearly resolved.

The average particle density is determined by measuring the mean frequency shift for a population of particles in at least two carrier solutions having different densities. Figure 2 shows the mean frequency shift for 1.51  $\mu$ m polystyrene particles in pure H<sub>2</sub>O, 25% D<sub>2</sub>O: 75% H<sub>2</sub>O, and pure D<sub>2</sub>O. The extrapolated  $x$  intercept yields the solution density that is equal to the particle density, at which point the particle differential mass is zero. The measured polystyrene density is  $1.0507 \pm 0.0004$  g/cm<sup>3</sup>, which is in agreement with the nominal value of 1.05 g/cm<sup>3</sup>. It is noteworthy that the density measurement does not require the frequency response of the SMR to be calibrated since the  $x$  intercept is independent of the units of the  $y$  axis (Fig. 2).

<sup>a)</sup>Electronic mail: scottm@media.mit.edu

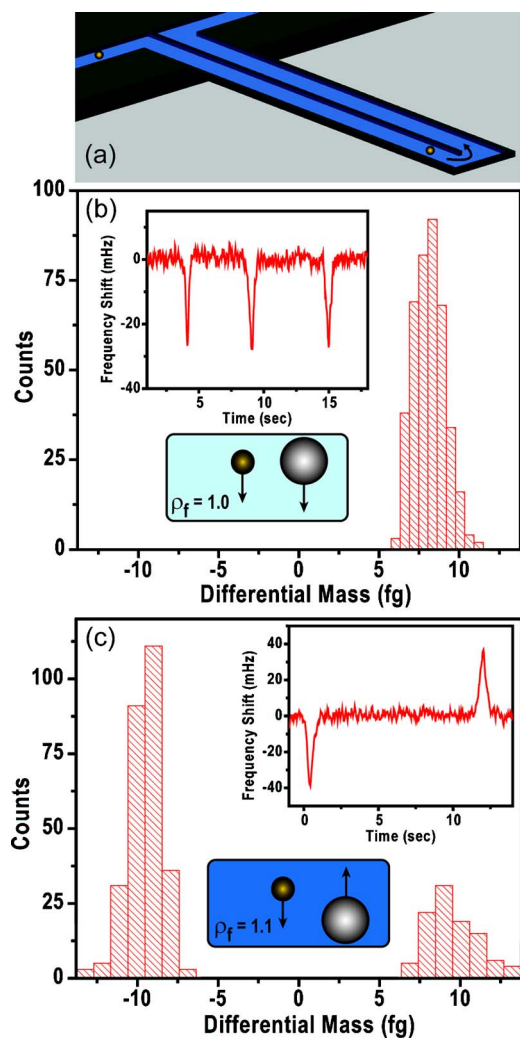


FIG. 1. (Color online) (a) Particles flow through the suspended microfluidic channel contained within the resonating cantilever (the channel is completely enclosed within the beam). (b) A mixture of 99.5 nm gold and 708.6 nm polystyrene nanoparticles are measured in PBS. The differential masses of both particles are positive and the mass histograms overlap. The inset shows the time course of the frequency signal as particles flow through the device, but each peak cannot be assigned to either gold or polystyrene. The schematic indicates that both particles have a positive differential mass since their densities are larger than that of the surrounding fluid. (c) The differential mass of gold in a 44% glycerol/H<sub>2</sub>O solution remains positive, but is negative for polystyrene, as immediately discerned from the time course data shown in the inset. The two histograms are now clearly distinct.

Such density measurements could have significant biological and diagnostic applications as well. As an example, the mean densities of *Escherichia coli* bacteria<sup>3</sup> and human red blood cells<sup>4</sup> were measured by weighing each sample in solutions of different densities. The inset of Fig. 2 shows the mean frequency shifts measured for *E. coli* and for human red blood cells suspended in various NaCl:HistoDenz<sup>5</sup> solutions. While HistoDenz was used to increase solution density, the solutions were prepared to maintain osmolality at 290 mOsm to minimize osmotic effects that could affect cell size and density. Extrapolation of a linear fit provides a mass density of *E. coli* of  $1.160 \pm 0.001$  g/cm<sup>3</sup> and a mass density of human red blood cells of  $1.139 \pm 0.003$  g/cm<sup>3</sup>. Both the *E. coli* and the human red blood cell densities are slightly higher than what have previously been reported,<sup>6,7</sup> which may be explained by differences in cell age, storage conditions, and solution tonicity, which are all known to significantly affect cell density.

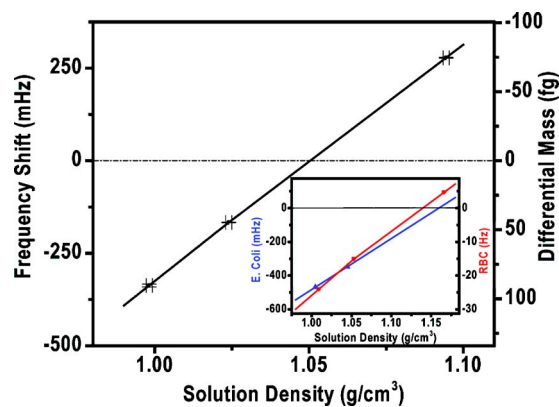


FIG. 2. (Color online) The density of 1.51  $\mu\text{m}$  polystyrene particles is determined by making frequency shift measurements in three solutions of differing densities at 20 °C. Each average mass value is obtained from 300–600 individual particle mass measurements. The  $x$  intercept yields the particle mass density. The densities of *E. coli* bacteria and of human red blood cells were also measured (inset). The sample solution densities can be quantified from the change in the baseline frequency ( $10\,702.7$  Hz g<sup>-1</sup> cm<sup>3</sup>) that occurs when water ( $\rho_f \approx 0.9982$  g/cm<sup>3</sup> at 20 °C) is replaced with the sample solution.

The precision in the density measurement is influenced by the choice of carrier solutions. For example, while we have measured the density of denser particles (e.g., silica,  $\rho_p \approx 2$  g/cm<sup>3</sup>) in H<sub>2</sub>O ( $\rho_f \approx 1.0$  g/cm<sup>3</sup>) and D<sub>2</sub>O ( $\rho_f \approx 1.1$  g/cm<sup>3</sup>), precision is slightly degraded since the longer extrapolation to the  $x$  intercept amplifies uncertainty. A two-point density measurement for polystyrene ( $\rho_p \approx 1.05$  g/cm<sup>3</sup>) in H<sub>2</sub>O and D<sub>2</sub>O yields an uncertainty in density of about 0.1% given that the mean differential mass can be measured to within 0.3%. This uncertainty increases to 1.4% and 3.7% for particles with densities of 1.5 and 2 g/cm<sup>3</sup>, respectively. This tendency can be countered by using fluids with a larger density difference. For example, using CsCl solutions ( $\rho_f \approx 1.8$  g/cm<sup>3</sup>) and ethanol ( $\rho_f \approx 0.79$  g/cm<sup>3</sup>), we estimate measurement uncertainties of 0.05% for polystyrene density and only 1.5% for a particle density of 4.5 g/cm<sup>3</sup>. When compared to density gradient centrifugation, which is currently the only established technique for particle density determination, our method is about an order of magnitude more sensitive, while avoiding the laborious and often error-prone preparation of a well defined density gradient.<sup>8</sup>

To demonstrate that this method can be used for polydisperse samples, we created a sample containing five distinct sizes of polystyrene spheres with diameters ranging from 670 nm to 1.9  $\mu\text{m}$ . The particles were weighed in water and the average density for each particle size was determined by repeating the experiment in heavy water (D<sub>2</sub>O). The volume/size of particles is inferred from the mass and density measurements, as described above.<sup>9</sup> Figure 3 shows the resulting size histograms for the mixture. The inset of Fig. 3 shows the density plots for the three smallest particles. The average particle sizes measured with the resonator agree with the nominal values.<sup>10</sup> For each size the standard deviation in diameter is  $\sim 4\%$ , slightly exceeding the specification (3%). The discrepancy may be caused by variations in the longitudinal position as the particles pass through the 8  $\mu\text{m}$  wide channel at the end of the cantilever.<sup>1</sup> Reducing the ratio of the channel width to the cantilever length or changing the resonator format to a doubly clamped beam would mitigate

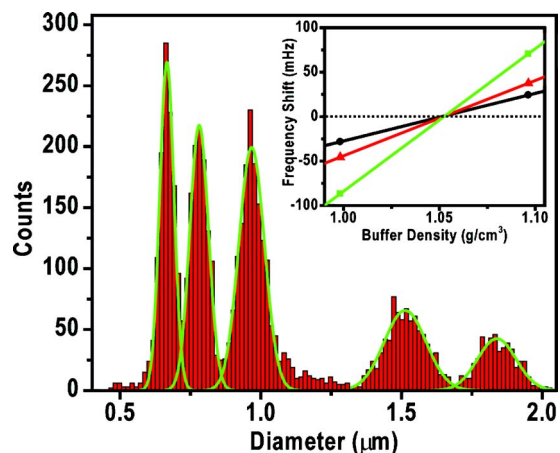


FIG. 3. (Color online) Size histogram for a mixture of polystyrene particles of five distinct sizes. The mass histograms of all five particles were acquired during a single run counting 5398 individual events. The five histograms were fitted to Gaussians (solid green lines). The densities of the particles were determined by measuring the same mixture in  $D_2O$ . The density measurement showing the  $x$  intercept is shown (inset) for the three smaller particles. Mean sizes of  $670 \pm 30$  nm,  $780 \pm 30$  nm,  $970 \pm 40$  nm,  $1.51 \pm 0.08$   $\mu\text{m}$ , and  $1.89 \pm 0.06$   $\mu\text{m}$  were measured. Their respective densities were  $1.050 \pm 0.001$ ,  $1.051 \pm 0.001$ ,  $1.051 \pm 0.001$ ,  $1.052 \pm 0.001$ , and  $1.049 \pm 0.001$   $\text{g}/\text{cm}^3$ .

this effect. Variations in density within a particle population will also produce variations in inferred size. It is unclear whether this effect influences the data in Fig. 3, but it should be considered when measuring porous particles or inhomogeneous samples.

The sample highlighted in Fig. 3 was constructed so that the number concentration for each particle size was uniform, yet the measured particle count is skewed toward smaller particles. We observe this effect to progress with time, suggesting a faster settling time for larger particles in the fluidic tubing that feeds the sensor. This artifact can be minimized by reducing tubing and channel lengths, increasing the feed flow rate and sonication, ultimately enabling the precise measurement of particle concentration.

The SMR's particle measurement capabilities are a valuable complement to light scattering and other particle sizing methods currently used in numerous industrial and research applications.<sup>2</sup> Of particular note is the SMR's ability to directly measure the mass/density of individual particles with high precision and accuracy. These capabilities provide a counterpoint to optical "ensemble" techniques, such as laser diffraction, which are sensitive to the shape and optical properties of the target particles and which for some samples are prone to artifacts and irreproducibility.<sup>2,11</sup> In its current incarnation, the SMR excels for particles from  $\sim 50$  nm to  $\sim 10$   $\mu\text{m}$ . Future improvements in mass resolution may al-

low the measurement of particles down to the  $\sim 10$  nm scale. The SMR's ability to measure particle density is unique among particle size analyzers and may be applied to applications such as the measurement of porosity and capacity of drug-loaded microspheres, the characterization of engineered porous silica used in coatings, slurries, and optoelectronics, and examination of the structure of submicron-sized particles.

In biology and medical diagnostics, correlations of mass and density with disease and other physiological states have been established, for example, in the various stages of malaria,<sup>12</sup> but the measurement techniques<sup>13–15</sup> remain laborious. The SMR provides a sensitive approach to examine the growth of biological mass during mitosis and other processes on the single-cell level if trapping capabilities are implemented in the resonator. It may also be possible to distinguish among species of bacteria or pathogens by varying the density of the carrier fluid in a manner analogous to Fig. 1.

We acknowledge financial support from the National Institutes of Health (NIH) Cell Decision Process Center Grant, the Institute for Collaborative Biotechnologies from the U.S. Army Research Office, and a National Science Foundation (NSF) Small Business Innovation Research award. M.G. acknowledges support from the Natural Sciences and Engineering Research Council of Canada (NSERC) through a post-doctoral fellowship.

<sup>1</sup>T. P. Burg, M. Godin, S. M. Knudsen, W. Shen, G. Carlson, J. S. Foster, K. Babcock, and S. R. Manalis, *Nature* (London) **446**, 1066 (2007).

<sup>2</sup>A. Jilavenkatesa, S. J. Dapkunas, and L. S. H. Lum, *Particle Size Characterization*, NIST Recommended Practice Guide (NIST Special Publication) (U.S. Government Printing Office, 2001), Vol. 960, p. 1.

<sup>3</sup>Invitrogen One Shot with ampicillin resistance.

<sup>4</sup>Research Blood Components.

<sup>5</sup>Sigma-Aldrich.

<sup>6</sup>W. W. Baldwin, R. Myer, T. Kung, E. Anderson, and A. L. Koch, *J. Bacteriol.* **177**, 235 (1995).

<sup>7</sup>R. C. Leif and J. Vinograd, *Proc. Natl. Acad. Sci. U.S.A.* **51**, 520 (1964).

<sup>8</sup>N. Mohandas, A. Johnson, J. Wyatt, L. Croisille, J. Reeves, D. Tycko, and W. Groner, *Blood* **74**, 442 (1989).

<sup>9</sup>A mass sensitivity of  $-268$  ag/mHz was determined for this device by measuring the average frequency shift for a population of  $1.51$   $\mu\text{m}$  National Institute of Standards and Technology (NIST) polystyrene size standards (Bangs Laboratories) of known differential mass in water at  $20$   $^\circ\text{C}$ .

<sup>10</sup>Bangs Laboratories.

<sup>11</sup>D. J. Burgess, E. Duffy, F. Etzler, and A. J. Hickey, *AAPS J.* **6**, 20 (2004).

<sup>12</sup>K. J. Kramer, S. C. Kan, and W. A. Siddiqui, *J. Parasitol.* **68**, 336 (1982).

<sup>13</sup>B. R. Robertson, D. K. Button, and A. L. Koch, *Appl. Environ. Microbiol.* **64**, 3900 (1998).

<sup>14</sup>C. G. Marxer, M. C. Coen, T. Greber, U. Greber, and L. Schlappbach, *Anal. Bioanal. Chem.* **377**, 578 (2003).

<sup>15</sup>T. Zhou, K. A. Marx, M. Warren, H. Schulze, and S. J. Braunhut, *Bio-technol. Prog.* **16**, 268 (2000).